Effects of Cross-Linking on the Morphology of Structured Latex Particles. 2. Experimental Evidence for Lightly Cross-Linked Systems

Yvon G. Durant, Eric J. Sundberg,† and Donald C. Sundberg*

Polymer Research Group, Department of Chemical Engineering, University of New Hampshire, Durham, New Hampshire 03824

Received April 17, 1996; Revised Manuscript Received October 11, 1996[⊗]

ABSTRACT: Elastic forces within very lightly cross-linked seed latex particles are able to compete with interfacial forces to influence latex particle morphology. At higher levels of cross-linking the elastic forces dominate those at the interfaces. PMMA seed latices were prepared at (nominally) 0, 0.015, 0.10, and 0.2 mol % (based on monomer) EGDMA cross-linking agent and subsequently swollen with styrene at a stage ratio of about 235%. After reaction, transmission electron micrographs of microtomed sections of the second stage latex particles showed that as little as 0.015% EGDMA (over 9000 repeating units between cross-links) began to shift the particle morphology from inverted core−shell (i.e. the second stage PS in the core) toward core−shell. At 0.2% EGDMA the particles were essentially of the core−shell morphology. Comparisons with predictions from a Gibbs free energy analysis of the effect of seed latex cross-linking on particle morphology are presented and show agreement with the experimental results.

Introduction

The industrial production of emulsion polymers for application in impact resistant plastics, coatings, and other products involves composite latex particles. Such products derive their properties in part from the morphology of the particles, and in a significant number of instances either or both phases of these particles are cross-linked to some extent. Cross-linking of the seed latex particle is often done to impart specific physical properties to the final product, as in ABS polymers, and also to influence the morphology of the structured particle. Several authors have reported the influence of cross-linking on particle morphology at full conversion through an experimental approach.[1−8] Recently,[9] we have shown via a computational approach that seed latex cross-linking can have a dramatic effect on the latex morphology, even at very low levels of cross-linking. Due to the very strong elastic forces necessary to deform a seed latex particle, the interfacial tensions at the particle surfaces (internal and external) are quite easily relegated to play a secondary role in determining the morphology. Thus it has been of interest for us to investigate the interplay of elastic forces and interfacial tensions from both a theoretical and experimental perspective. The purpose of this paper is to provide experimental observations to compare with predictions from our above referenced thermodynamic analyses.

Experimental Section

Materials. All water used was double distilled and deionized and will be referred to as DI water. Methyl methacrylate (MMA) (Aldrich No. M5,590−9) and styrene (Sty) (Aldrich No. S497−2) monomers were cleaned of their inhibitor. This was accomplished by a liquid−liquid extraction with three separate fractions of NaOH (Baker) (1 M in DI water) followed with three sequential extractions with DI water and drying over $MgSO_4$ (Aldrich No. 24,697−2). Ethylene glycol dimethacrylate (EGDMA) (Aldrich No. 33,568−1), sodium dodecyl sulfate (SDS) (Aldrich No. 86,201−0), $NaHCO_3$ (Aldrich No. 34,094−4), and potassium persulfate (KPS) (Aldrich No. 21,622−4) were used "as is" with no further purification.

General Approach. We decided to work on a PMMA seed, cross-linked with EGDMA, because of the good reactivity of the second vinyl function of EGDMA and its chemical similarity with MMA. Styrene as a second stage monomer was chosen in part because of the natural contrast between PS and PMMA in the electron microscope. We first developed a series of experiments to produce cross-linked seeds of low cross-linking density (0.1, 0.2, 0.5, 1, 2% EGDMA). The second stage was polymerized at stage ratios of 30, 50, and 100, and 200%. Electron microscope observation of these particles proved to be nonconclusive due in part to the small amount of second phase, except for the 200% swelling experiment (see XL3, Table 2). We redesigned our experiments with higher stage ratios and larger seed particle sizes, but with lower cross-linking densities, as guided by our theoretical calculations. This second set of experiments is presented here.

Latex Preparation. The seed latices were made in a 1.2 L double-jacketed reactor, with a mechanical stirrer and a condenser, and produced under a nitrogen atmosphere. Oxygen was stripped from the DI water with a nitrogen purge for 30 min. The first three seeds were "soap free" latices made by initiation via KPS at 80 °C. The monomer/water mixture was stirred at 600 rpm which was then reduced to 500 rpm, 7 min after the introduction of the initiator solution (4% in DI water). The fourth seed was made by classical surfactant stabilization at 60 °C, under a lower stirring rate of 200 rpm. In these experiments the EGDMA was diluted in a portion of the MMA and fed continuously over the first hour of the polymerization for experiments XL1 and XL2, since 90% of the batch polymerization of the MMA was complete after 1 h at 80 °C. The fourth seed, XL3, was prepared by continually feeding both the MMA and EGDMA over a period of 4 h. These semicontinuous polymerizations were carried out in accordance with the software developed by Guillot[10−12] which models the polymerization kinetics of cross-linked latices and predicts the conditions for achieving cross-link homogeneity throughout the polymerization process and across the particle. The seed latices were kept at their polymerization temperature for a longer time than necessary to complete the thermal dissociation of the initiator.

The second stage polymerizations were carried out in a 250 mL glass reactor equipped with a mechanical stirrer and a condenser, submerged in a water bath, and operated under a nitrogen atmosphere. Before the start of the second stage polymerization, the styrene was preswollen into the seed particles for 2 h. Then the batch polymerization was carried out at 60 °C. All the experimental parameters are reported in Table 1, while Table 2 provides the principal characteristics of these latices.

† Department of Biochemistry, Molecular Biology and Cell Biology, Northwestern University, Evanston, IL.

⊗ Abstract published in *Advance ACS Abstracts,* January 1, 1997.

S0024-9297(96)00568-2 CCC: $14.00

Table 1. Recipe for the Seed and Second Stage Polymerizations

	XL0 no EGDMA	XL1 0.015% EGDMA	XL2 0.1% EGDMA	XL3 0.2% EGDMA
		Seed Recipe		
MMA (g)	113.9	114	114	100.61
DI water (g)	1079.8	1075.5	1080.1	950.37
KPS (g)	0.6328	0.6329	0.6410	0.5001
$NaHCO_{3\,(g)}$	0.1984	0.1988	0.1973	0.5077
SDS (g)	0	0	0	0.5050
EGDMA (g)	0	0.0322	0.2257	0.4493
EGDMA addition mode		starve feed 1 h 1% in MMA	starve feed 1 h 1% in MMA	starve feed 4 h 0.28% in MMA
polymerization time (h)	8	13	12	6
polymerization temp (°C)	80	80	80	60
		Second Stage Recipe		
seed latex (g)	85.2	94.7	94.7	101.71
styrene (g)	16.2	18.0	18.0	20.0
DI water (g)	32.7	36.9	39.6	27.83
KPS (g)	0.0691	0.0766	0.0766	0.5037
$NaHCO_3$ (g)	0.0143	0.0199	0.0154	0.5076
SDS (g)	0	0	0	0.5076
polymeirzation time	8	6	8	5

Table 2. Principal Characteristics of the Latices

	XL0	XL1	XL2	XL3
seed particle size (nm), approx	250 (tubidity)	280 (TEM)	300 (TEM)	90 (TEM)
seed solid content (wt %)	8.39	8.82	9.10	9.61
stage ratio (vol %)	247	235	229	224
M_c/M	∞	9347	1330	590
second stage solid content (wt %)	16.66	16.84	16.72	20.01
conversion of styrene (%)	94	93.5	93.6	100

Sample Preparation for Transmission Electron Microscopy (TEM). For a good analysis of the internal particle morphology, we microtomed and stained the latex samples. First a sample of the latex was allowed to dry at room temperature to form a solid disk. The disk was broken into chips, and one or two pieces were embedded in epoxy (Fluka Chemika, Epon 45345, 45346, 45347, 45348) at room temperature, allowed to stand for 48 h, and then raised to 60 °C for 6 h to cure the epoxy. The samples were rough-trimmed first, then microtomed with a glass knife, and finally microtomed with a diamond knife to a slice thickness of 65−70 nm. The thin slices were collected on a copper grid and stained with ruthenium tetraoxide. RuO_4 was made from RuO_2 (1 g of $NaIO_4$ in 25 mL of ice cold DI water, add 0.15 g of $RuO_2 \cdot 2H_2O$) and stored at 6 °C for a maximum of 1 month. The epoxy/latex thin slices were exposed to the RuO_4 vapors for 2 h at room temperature. For our TEM observations we used a Hitachi 600 microscope at 75 keV.

Discussion

When we consider a cross-linked seed latex particle which has been deformed due to the presence of a second phase, there will be elastic forces which result in a given amount of free energy, G_e, stored in the particle. This energy combines with that of the interfacial free energy to yield the total free energy of the particle, G. This can be expressed as

$$G = G_s + G_e + G^0 \tag{1}$$

where G is the total free energy of the particle, G_s is the interfacial energy, and G^0 is the reference state energy. Equation 1 differs from that applied to our previous free energy analyses of latex particle morphology only by the term G_e, and here we follow our previous approach in which we consider the differences between G for two varieties of particle structures. In this paper we will restrict our considerations to core−shell (CS) and inverted core−shell (ICS).

The elastic forces are dependent on four dominant parameters:

- T, the temperature
- M_c/M, the number of repeating units between cross-links
- α, the displacement gradient tensor
- b, the stiffness of the chain

The elastic term, G_e, is considered to be a function of M_c, α, b, and T. According to the fundamental thermodynamic definitions, stored energy $= E = \int f \, dx = U$ and at constant temperature and pressure $G_e = U$. Here U is the internal energy.

As presented earlier,[9] we derived from the statistical mechanics of polymer chains[13,14] that

$$E = \frac{\rho R T}{M_c}\left(1 - 2\frac{M_c}{M_w}\right)\left[(\alpha^2 + 2\alpha^{-1} - 3)\frac{1}{2}b + (\alpha^4 + 2\alpha^{-2} - 3)\frac{1}{20}\frac{M}{M_c}b^2 + (\alpha^6 + 2\alpha^{-3} - 3)\frac{11}{1050}\left(\frac{M}{M_c}\right)^2 b^3\right] \tag{2}$$

where ρ is the density of the polymer, R is the gas constant, T is the temperature, M_c is the molecular weight between cross-links, M_w is the molecular weight of the un-cross-linked chain, and M is the molecular weight of the monomer. When applied to the case of one occlusion in a cross-linked sphere, or inverted core−shell (ICS), eq 2 needs to be integrated over the specific geometry. Figure 1 shows a geometric representation of the initial sphere and a postformed inverted core−shell particle. r_s is the radius of the original sphere (cross-linked seed),and r_o is the radius of the occlusion. The radial distance r is then transposed in the expanded sphere to a new radius r'. For a layer of thickness dr

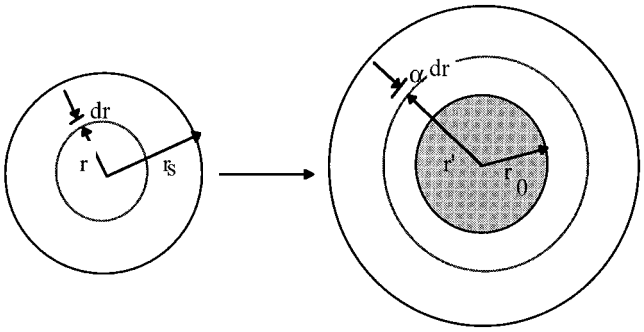

Figure 1. Geometrical representation of the expansion of the seed particle of radius r_s to an inverted core−shell (ICS) with a core radius r_0. r' represents the diplacement of an arbitrary point in the seed particle represented by r. dr and α dr are the corresponding layer thicknesses.

at radius r we have the following energy based on an integration of eq 2:

$$G_e = \int_0^{r_s} E 4\pi r^2 \, dr = 4\pi \frac{\rho R T}{M_c}\left(1 - 2\frac{M_c}{M_w}\right)\int_0^{r_s}\left[(\alpha^2 + 2\alpha^{-1} - 3)\frac{1}{2}b + (\alpha^4 + 2\alpha^{-2} - 3)\frac{1}{20}\frac{M}{M_c}b^2 + (\alpha^6 + 2\alpha^{-3} - 3)\frac{11}{1050}\left(\frac{M}{M_c}\right)^2 b^3\right] r^2 \, dr \quad (3)$$

with the displacement tensor being a function of r, as follows

$$\alpha = \left(1 + \left(\frac{r_0}{r}\right)^3\right)^{-2/3} \quad (4)$$

It is then possible to numerically calculate the stored energy, G_e, from eqs 3 and 4. We have solved eqs 2 and 3 by creating two master curves for G_e which depend on r_s and r_0. This is described in a previous publication.[9]

The expression of the difference of surface free energy between an ICS and a CS is well-known and has been published several times.[15−23]

$$\Delta G_s = 4\pi[(r_s^3 + r_0^3)^{2/3}(\gamma_{P1/W} - \gamma_{P2/W}) + \gamma_{P1/P2}(r_0^2 - r_s^2)] \quad (5)$$

Here, $\gamma_{P1/W}$ is the interfacial tension at the polymer 1 (seed polymer)/water interface, $\gamma_{P2/W}$ is that at the polymer 2/water interface, and $\gamma_{P1/P2}$ is that between the two polymers. Note that the reference CS particle has no elastic energy, as only the seed polymer is cross-linked. Thus the difference in total free energy ΔG between an ICS and a CS is

$$\Delta G = \Delta G_e + \Delta G_s = G_e + \Delta G_s \quad (6)$$

Given values of the various interfacial tensions, the seed latex particle size (r_s) and the amount of second stage polymer (equivalently r_0 for the case of a CS), one can use eqs 5 and 6 to determine whether the ICS structure is thermodynamically favored over a core−shell arrangement. Since the CS was taken as the reference state, positive values of ΔG in eq 6 predict that the CS is preferred, while negative values predict that an ICS is preferred.

As before,[9] we find it useful to compare these free energies with those that would exist if the particle were simply a core−shell (CS), with the core being the seed polymer. If we consider the situation in which we can only have either a CS or an ICS particle morphology, we can observe the total particle energy plotted against the cross-link density (M_c/M) with a reference line indicating the energy of the CS shell arrangement. Thus when ΔG is below that line, the ICS structure has less energy than the CS structure. When ΔG is above the reference line, the ICS structure requires more energy than the CS structure and the particle morphology will be predicted to be CS. This is illustrated graphically in Figure 2 for a PMMA seed latex of 275 nm diameter, cross-linked with EGDMA to yield various levels of cross-linking, and with PS as a second stage at a stage ratio of 235% (these values represent the averages of the experimental variables for XL0−XL3). Here the CS reference line is at an energy level of 0 fJ (fJ = femtoJoule = 10^{-15} J). The curved lines represent the total energy calculated from eq 6 as a function of the cross-link level of the seed PMMA. From these curves one can see that for M_c/M values greater than about 3000 (representing an EGDMA level of about 0.044%) the preferred particle structure is an ICS. At higher levels of cross-linking the situation is reversed and the CS arrangement is preferred.

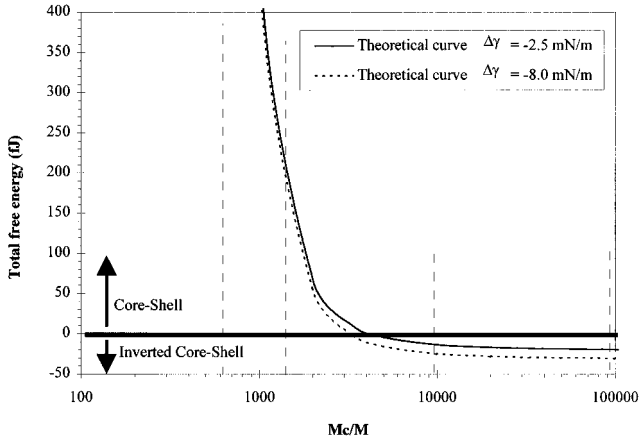

Figure 2. Total energy (ΔG) versus seed latex cross-link level (M_c/M) for chain stiffness $b = 7$ and ($\gamma_{P1/W} - \gamma_{P2/W}$) = −2.5 and −8 mN/m. Experimental conditions are noted at $M_c/M = \infty$, 9347, 1330, and 590, for XL0, XL1, XL2, and XL3, respectively.

The experiments described earlier are positioned in Figure 2 by the dotted vertical lines. The case for the un-cross-linked seed, experiment XL0, is positioned at the far right hand side of the plot since the M_c/M value in this case is infinity. The values of M_c/M for experiments XL1, XL2, and XL3 were determined by assuming that the EGDMA created cross-links with 75% effectiveness (i.e. 25% of the pendent vinyl group does not react), and that the cross-linking was uniform throughout the seed polymer. Thus M_c/M is given as 1/(0.75[EGDMA]) when [EGDMA] is expressed as a fraction. Thus experiment XL1 had M_c/M = 1/(0.000142 × 0.75) = 9347, while XL2 and XL3 had M_c/M's of 1330 and 590, respectively.

As shown in eq 5, we need values of $\gamma_{P1/P2}$ and ($\gamma_{P1/W} - \gamma_{P2/W}$) in order to compute ΔG_s and ΔG (eq 6). $\gamma_{P1/P2}$ was taken as 1.7 mN/n in accordance with our previous work,[21] neglecting any potential effect of PMMA cross-linking on the interfacial tension between the two polymers. At high concentrations (approaching CMC) of SDS in the aqueous phase, ($\gamma_{P1/W} - \gamma_{P2/W}$) for the PMMA/PS system has been measured by us[21] to be about −2.5 mN/m. This characterizes experiment XL3 of Table 1. For experiments XL0 through XL2 we do not have individual values of $\gamma_{P1/W}$ and $\gamma_{P2/W}$. This is

because both the seed PMMA and second stage PS have ionic end groups (derived from initiator dissociation) at their aqueous interfaces and there are no reliable published data for such conditions that we are aware of. For pure polymer against water, ($\gamma_{P1/W} - \gamma_{P2/W}$) is roughly[21] (19 − 31) mN/m = −12 mN/m. With a high level of ionic end groups at the PS polymer surface (i.e. at a surface charge density of 5 μC/cm^2 as measured for the PS latex), we have estimated[24] the $\gamma_{P2/W}$ to be about 23 mN/m. The reduction of γ due to end groups for the PMMA seed polymer is more difficult to estimate since the end groups are due to reactions which took place during seed latex preparation. During the second stage polymerization the surface end groups for the PMMA are fixed and if the PMMA were to engulf the second stage PS for the ICS structure, those end groups would become more spread out than they were on the seed particle surface. We have developed a computational scheme[25] for estimating the value of $\gamma_{P1/W}$ under these conditions, and for an initial (prior to second stage polymerization) charge density of 5 μC/cm^2 on the seed, we estimate that $\gamma_{P1/W}$ is about 15 mN/m when the PMMA engulfs the second stage polymer. These calculations were obtained from our UNHLATEX_EQMORPH software which allows for the calculation of the various interfacial tensions over a wide variety of conditions. The end group calculations are quite detailed and will be left to a future publication. Given all the above, we estimate that for experiments XL0, XL1, and XL2 the ($\gamma_{P1/W} - \gamma_{P2/W}$) value is about (15 − 23) = −8 mN/m. While it may be somewhat less negative than this value, it is not likely to be more negative. Thus, in Figure 2 we have presented two ΔG curves, one for ($\gamma_{P1/W} - \gamma_{P2/W}$) = −8 mN/m representing experiments XL0 through XL2 and one for −2.5 mN/m representing experiment XL3. One further note about these curves is that the "stiffness parameter" necessary to use eq 2 has been taken to be $b = 7$, which is reported to be characteristic of PMMA.[11]

Inspection of Figure 2 shows that we would expect XL0 and XL1 to be ICS and the other two to be CS particles. The experimental evidence is shown in Figure 3a−d. These micrographs are TEM's of microtomed sections of the representative particles stained with ruthenium tetraoxide so that the dark phase is PS and the light phase is PMMA. In Figure 3a it is clear that the PS has become located in the interior of the particle. Although the PS does not appear to exist as a single core, it is clear that it is completely engulfed with the PMMA, much like an ICS. Cross-linking the seed PMMA with EGDMA at a level of 0.015% based on MMA monomer causes the PS to be moved toward the outer edge of the particle and more PMMA to exist within the central part of the particle, as shown in Figure 3b. This is a dramatic effect at a very low level of cross-linking agent. At an EGDMA level of 0.10%, the microtomed sections show that nearly all of the PS exists at the periphery of the particle and forms a structure approximating a CS arrangement, as in Figure 3c. Further increase of the EGDMA level to 0.2% results in apparently more uniform CS particles, as shown in Figure 3d. Due to possible overexposure of the thinner part of the image area at the center of the photo, the reader is directed to observe particles away from the center. Here the TEM was obtained by observing the whole particle (stained as before but not microtomed) in the microscope. Thus we have obtained good agreement between the predictions and the experiments, and these results verify the conclusion reached in our earlier paper[9] that latex particle morphology is **very** sensitive to the level of cross-linking of the seed polymer.

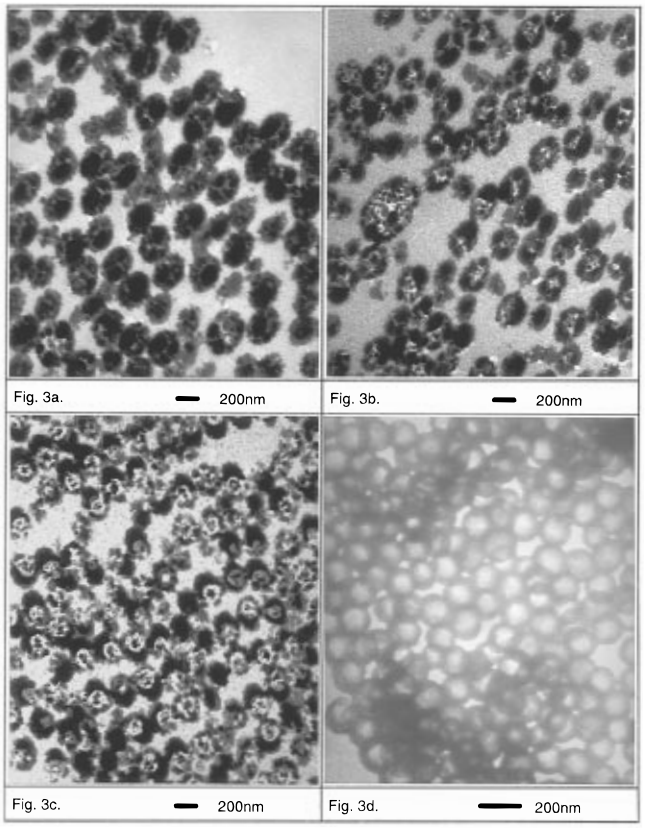

Figure 3. Transmission electron micrographs of experiments (a) XL0, (b) XL1, (c) XL2 and (d) XL3 at 75 keV. All samples were stained with RuO4. Samples XL0, XL1, and XL2 were microtomed and magnified at 20000×. Sample XL3 is the whole particle, magnified 50000×.

As noted in Figure 2, the ΔG curves were calculated for $b = 7$ and the M_c/M values for the experiments were determined by assuming that 75% of the EGDMA was incorporated in cross-links. Although not presented here for the sake brevity, we have constructed similar plots for $b = 1$ (a freely rotating chain) and EGDMA efficiency of 100%. Under these conditions the comparison between theory and experiment yields the same results as presented above, thus giving us added confidence in our interpretation of the reasons for the changes seen in Figure 3.

Concluding Remarks

We supect that many of our industrial colleagues have for some time used seed latex polymer cross-linking as a tool to help achieve CS particle structures. It is also noted that unintentional cross-linking can occur in seed latex preparation via chain transfer to polymer, as in acrylic polymers. Combining the computational approach suggested in the first paper of the series[9] with the experimental results reported here, it is clear that very low levels of cross-linking can singularly be responsible for dramatic shifts in particle morphology, particularly when the seed polymer is significantly more polar than the second stage polymer. The computations offer one the ability to determine the cross-linking level that creates the balance between interfacial and elastic forces which determine equilibrium particle morphology. These calculations are dependent upon all of the pa-

rameters which affect interfacial tensions (e.g. polymer polarity, surfactant type and level, end groups, etc.) and thus can reflect practical conditions of latex manufacture.

Acknowledgment. We are grateful for the financial support provided by the University of New Hampshire and the Centre National de la Recherche Scientifique (LCPP Lyon, France). We also wish to thank Dr. Jean Guillot for allowing us to use his software program to calculate the EGDMA addition feed rate for the preparation of the seed latices and Vicki Dycewicz for the microtoming and electron microscopy work.

References and Notes

(1) Lee, S.; Rudin, A. *Macromol. Chem. Rapid Commun.* **1989**, *10*, 655.
(2) Lee, S.; Rudin, A. *J. Polym. Sci., Part A: Polym. Chem.* **1992**, *30*, 2211.
(3) Jönsson, J.-E. L.; Hassander, H.; Jansson, L. H.; Törnell, B. *Macromolecules* **1991**, *24*, 126.
(4) Rosen, S. L. *J. Appl. Polym. Sci.* **1973**, *17*, 1805.
(5) Merkel, M. P.; Dimonie, V. L.; EL-Aasser, M. S.; Vanderhoff, J. W. *J. Polym. Sci., Part A: Polym. Chem.* **1987**, *25*, 1755.
(6) Hourston, D. J.; Satgurunathan, R.; Varnma, H. *J. Appl. Polym. Sci.* **1986**, *31*, 1955.
(7) Hourston, D. J.; Satgurunathan, R.; Varnma, H. *J. Appl. Polym. Sci.* **1987**, *33*, 215
(8) Vanderhoff, J. W.; Sheu, H. R.; El-Aasser, M. S. *Scientific Methods for the Study of Polymer Colloids and Their Applications*; NATO ASI series C; Kluwer Academic Publishers: Boston, 1990; Vol. 303, p 529.
(9) Durant, Y. G.; Sundberg, D. C. *Macromolecules* **1996**, *29*, 8466.
(10) Mathey, P.; Guillot, J. *Polymer* **1991**, *32* (5), 934.
(11) Guillot, J. *Makromol. Chem. Macromol. Symp.* **1990**, *35−36*, 269.
(12) Guillot, J. *Comput. Chem. Eng.* **1993**, *17*, S189.
(13) Schultz, J. M. *Polymer Materials Science*; Prentice-Hall: Englewood Cliffs, NJ, 1974; pp 306−316.
(14) Flory, P. J. *Statistical mechanics of chain molecules*; John Wiley and Sons: New York, 1969; p 35−42.
(15) Berg, J.; Sundberg, D. C.; Kronberg, B. *J. Polym. Mater. Sci. Eng.* **1986**, *54*, 367.
(16) Berg, J.; Sundberg, D. C.; Kronberg, B. *J. Microencapsulation* **1989**, *6*, 327.
(17) Sundberg, D. C.; Cassasa, A. J.; Pantazopoulos, J.; Muscato, M. R.; Kronberg, B.; Berg, J. *J. Appl. Polym. Sci.* **1990**, *41*, 1425.
(18) Muscato, M. R.; Sundberg, D. C. *J. Polym. Sci., Polym. Phys. Ed.* **1991**, *29*, 102.
(19) Winzor, C. L.; Sundberg, D. C. *Polymer* **1992**, *33*, 3797.
(20) Winzor, C. L.; Sundberg, D. C. *Polymer* **1992**, *33*, 4269.
(21) Sundberg, E. J.; Sundberg, D. C. *J. Appl. Polym. Sci.* **1993**, *47*, 1277.
(22) Durant, Y. G.; Sundberg, D. C. *J. Appl. Polym. Sci.* **1995**, *57*, 1607.
(23) Sundberg, D. C.; Durant, Y. G. *Macomol. Symp.* **1995**, *92*, 43.
(24) Durant, Y. G. Ph.D. Thesis No. 8094, University Claude Bernard - Lyon I, France, 1994.
(25) Durant, Y. G.; Sundberg, D. C. Unpublished results.

MA960568L